
Volume 306, Issues 3–4
15 June 2011
ISSN 0012-821X
ELSEVIER
EARTH
& PLANETARY
SCIENCE LETTERS
Editors
Rick Carlson, Washington, DC
Peter B. deMenocal, Palisades, NY
T. Mark Harrison, Los Angeles, CA
Gideon M. Henderson, Oxford, UK
Yanick Ricard, Lyon
P. Shearer, La Jolla, CA
Tilman Spohn, Berlin
Lars Stixrude, London

Earth and Planetary Science Letters 306 (2011) 163–174

Contents lists available at ScienceDirect

Earth and Planetary Science Letters

journal homepage: www.elsevier.com/locate/epsl

# Geology, Petrology and O and H isotope geochemistry of remarkably $^{18}O$ depleted Paleoproterozoic rocks of the Belomorian Belt, Karelia, Russia, attributed to global glaciation 2.4 Ga

I.N. Bindeman [a,*], N.S. Serebryakov [b]

[a] Department of Geological Sciences, 1272 University of Oregon, Eugene OR 97403, United States
[b] The Institute of Geology of Ore Deposits, Petrography, Mineralogy, and Geochemistry, Russian Academy of Sciences (IGEM RAS) Staromonetny per, 35, Moscow, Russia

ARTICLE INFO

*Article history:*
Received 15 December 2010
Received in revised form 23 March 2011
Accepted 24 March 2011
Available online 30 April 2011

Editor: R.W. Carlson

*Keywords:*
oxygen isotopes
hydrogen isotopes
snowball glaciation
slushball Earth
corundum
subglacial rifting

ABSTRACT

This paper deals with strongly $^{18}O$-depleted (down to −27.3‰ VSMOW) 1.9Ga Paleoproterozoic mid-grade metamorphic rocks found in the Belomorian Belt of Karelia (E. Baltic Shield). The protolith of these rocks is attributed to have been altered by glacial meltwaters during the world's first 2.4–2.3 Ga Paleoproterozoic "Slushball" glaciation, when Karelia was located near equatorial latitudes. We describe in detail three and report seven new localities with unusually depleted $^{18}O$ signatures that now span 220 km across the Belomorian Belt. Hydrogen isotope ratios measured in amphibole, biotite and staurolite also display remarkably low values of −212 to −235‰. Isotope mapping in the three best exposed localities has allowed us to identify the world's most $^{18}O$ depleted rock, located at Khitostrov with a $\delta^{18}O$ value −27‰. In Khitostrov samples, zircons have normal $\delta^{18}O$ detrital cores and low-$\delta^{18}O$ metamorphic rims. Mapping demonstrates that zones of $\delta^{18}O$ depletion occur in a concentric pattern 100–400 m in dimension, and each locality displays significant $\delta^{18}O$ and $\delta D$ heterogeneity on a meter to centimeter scale, characteristic of meteoric-hydrothermal systems worldwide. The zone of maximum $\delta^{18}O$ depletions usually has the highest concentration of metamorphic corundum, rutile, and zircon and also display doubled concentrations of insoluble trace elements (Zr, Ti, Cr, HREE). These results are explained by elemental enrichment upon mass loss during hydrothermal dissolution in pH-neutral meteoric fluid. Remarkably low-$\delta^{18}O$ and $\delta D$ values suggest that alteration could have only happened by glacial meltwaters in a subglacial rift zone. Many localities with $\delta^{18}O$ depletions occur inside metamorphozed 2.4 Ga gabbro-noritic intrusions, or near their contact with Belomorian gneisses, implying that the intrusions were driving meteoric hydrothermal systems during the known 2.4 Ga episode of Belomorian rifting. Given that the isotopically-depleted localities now spread over 200 km, the extent of the Karelian ice cap is estimated to be at least that large. Svecofennian 1.9 Ga metamorphism is seen to cause metamorphic recrystallization of hydrothermally-altered rocks into coarse-grained assemblages, and causing local metasomatism through devolatilization of the underlying hydrous low-$\delta^{18}O$ protolith, further depleting $\delta D$ via volatilization. This process led to gem-quality rubies and kyanites that preserve these remarkable $\delta^{18}O$ values in the geologic record.



## 1. Introduction

Silicate rocks with $\delta^{18}O$ values less than 5‰ SMOW require interaction with surface (sea or meteoric) waters, and those with less than 0‰ require exchange with meteoric (rain or snow) waters processed through vapor distillation (e.g. Hoefs, 2005). Because isotope fractionations between rocks and waters are small at temperatures more than 100–200 °C, $^{18}O$-depleted values closely approach those of altering meteoric water (e.g., Criss and Taylor, 1986). When $^{18}O$-depleted rocks are found in the geologic record, they can be used to make inferences about the $\delta^{18}O$ value of parental water, and the climate conditions appropriate for them. Such estimates may provide only the upper values for waters because water–rock interaction rarely proceeds to full equilibrium, and waters get rapidly shifted to heavier values. Very commonly, in major hydrothermal systems around the world: rift zones of Iceland, Skaergaard Intrusion, or calderas in Yellowstone and Kamchatka, the $\delta^{18}O$ values of hydrothermally-altered rocks are higher by up to 10‰, then is required by the equilibrium $\Delta^{18}O$(rock-unshifted water) (Bindeman et al., 2008; Hattori and Muelenbachs, 1982; Sturchio et al., 1990; Taran et al., 1988; Taylor and Forester, 1979). In this respect, the lowest-$\delta^{18}O$ value measured in rocks may correspond to the highest $\delta^{18}O$ of altering meteoric water.

Because $\delta^{18}O$ and $\delta D$ values of precipitation become progressively more negative with increasing latitude, altitude, and toward the center

* Corresponding author.
*E-mail address:* bindeman@uoregon.edu (I.N. Bindeman).

0012-821X/$ – see front matter © 2011 Elsevier B.V. All rights reserved.
doi:10.1016/j.epsl.2011.03.031

of large land masses (e.g. Dansgaard, 1964), the strongly negative $\delta^{18}O$ and δD values of subaerially-altered rocks have been occasionally used in the past to infer cold climate conditions. In particular Blattner et al. (1997), Dallai et al. (2001), and Bindeman et al. (2004) attributed these values to the effects of Phanerozoic glaciations. Many papers are published on Dabie Shan-Sulu ultra-high pressure metamorphic rocks and their protolith is interpreted to represent alteration by ca 750 Ma Neoproterozoic panglobal glaciation (Rumble and Yui, 1998; Zhao et al., 2002; Zheng et al., 2004). This paper deals with the origin of remarkably-depleted in $\delta^{18}O$ and δD (down to −27.3‰ and 235‰, respectively) Paleoproterozoic metamorphic rocks that belong to the Belomorian Belt in Karelia, the eastern part of the Baltic Shield (Fig. 1).

### 1.1. Geology of the Belomorian Belt

The Belomorian polymetamorphic complex is located between the Kola and Karelia Archean blocks (Fig. 1) and represents one of many Paleoproterozoic mobile belts around the world that underwent the 1.9–1.8 Ga metamorphism, in the process of accretion of the Nuna supercontinent (Zhao et al., 2002). From east to west, the Belomorian Belt is made of three complexes: the Khetolambina complex, representing metamorphosed oceanic crust and oceanic sediments, the Chupa complex, made of metagreywacke and siliciclastic metasediments of continental/shallow marine environments, and the Kovdozero complex representing the continental interior (Miller and Milkevich, 1995; Myskova et al., 2003). The formation of these three complexes and the Belomorian belt itself is attributed to the arc-Karelian continent collision at 2.6–2.7 Ga, based on dating the detrital zircons and their rims (Bibikova et al., 1994, 2001, 2004). The last metamorphic episode that affected the Belomorian Belt was the 1.9 Ga Svecofennian collisional event, which led to the final accretion of Karelia to Kola. In the mid-grade Belomorian Belt and in the Chupa gneiss complex in particular, rocks have undergone recrystallization but without much magmatism. Magmatic rocks of Svecofennian age are represented by minor migmatites in the host Chupa gneiss with 1.89 Ga zircon rims (Bibikova et al., 1994), regional intrusion of pegmatites of 1.9–1.8 Ga age (Skublov et al., 2010), and formation of metasomatites with corundum, having 1.89 Ga monazites and zircon rims (Bindeman et al., 2010; Serebryakov et al., 2007).

The lull in magmatic and metamorphic activity that characterized the world between 2.5 and 1.9 Ga (Condie et al., 2009) applies to Karelia, but with some important exceptions. At 2.4–2.5 Ga, Karelia and the Belomorian Belt have suffered rifting, and the main axis of rifting laterally coincided with the Chupa complex (Rybakov et al., 2000). Rifting was accompanied by the intrusion of predominantly high-Mg gabbros and basalts (Puchtel et al., 1997), the largest of which formed layered intrusions (Amelin et al., 1995; Sharkov et al., 1997). These gabbroids are locally known as 'druzite' bodies and they were variably metamorphosed during the Svecofennian stage, depending on their position in the Belomorian Belt (Stepanov, 1981). Weakly-metamorphosed basalts of this age have also been recently recognized among the Sumian sedimentary sequences (Svetov et al., 2004), and serve as an extrusive compositional analog to the druzites. It is important to stress that glacial rocks of Sariolian age (2.5–2.3 Ga) are found on the weakly (greenschist and lower grade) metamorphosed southwest portion of the Karelian craton in association with 2.4 Ga rifts (Bekker, in press; Ojakangas et al., 2001). The trace element geochemistry of 2.4 Ga high-Mg druzite bodies and

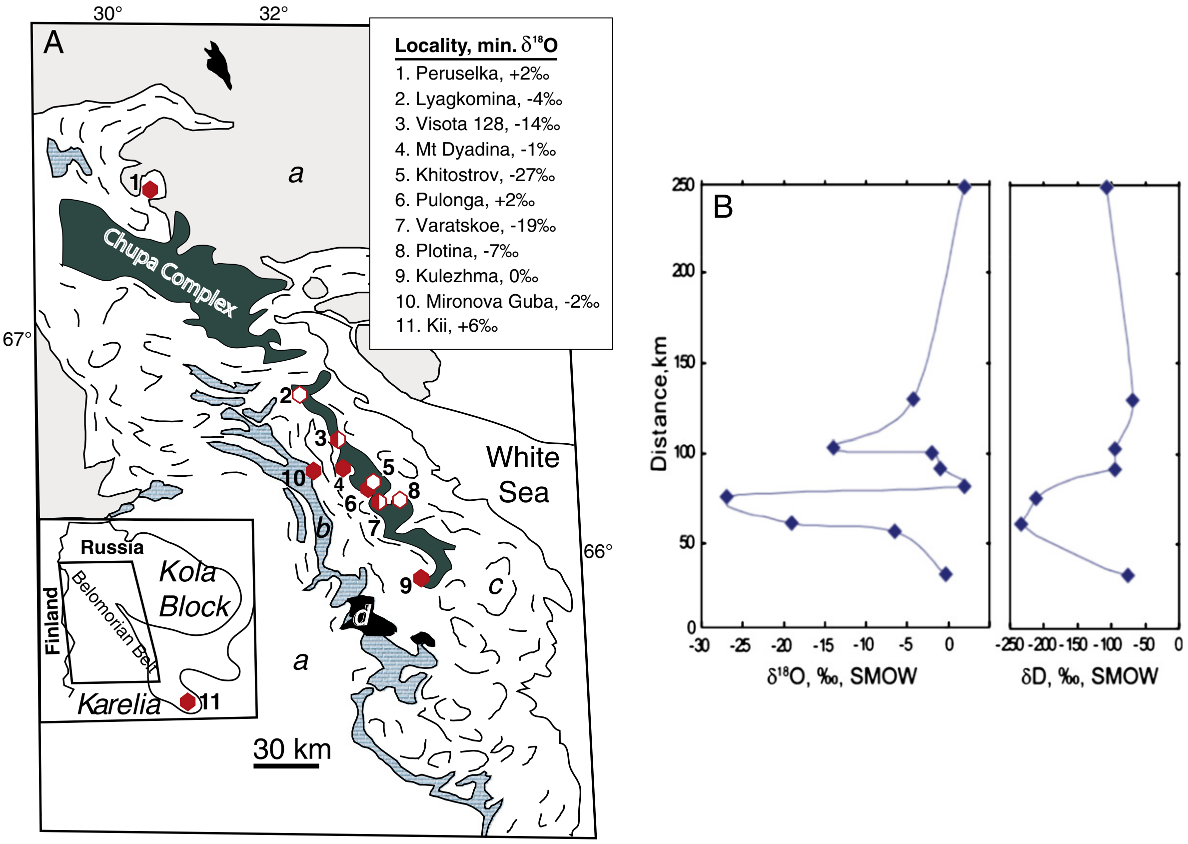


**Fig. 1.** A) Simplified geologic map of the Belomorian Belt with structural elements showing the position of the Paleoproterozoic–Neoarchean Chupa allochthonous nappe with studied localities with ultra low-$\delta^{18}O$ values, spanning 220 km (map is after Balagansky et al., 1986; Bibikova et al., 2004); (a) Karelian and Kola Archean blocks; (b) Archean metavolcanic and metasedimentary units; (c) other nappes of the Belomorian Belt; (d) gabbro-norite and layered intrusions (2.45–2.4 Ga). Maximum level of $\delta^{18}O$WR depletion is shown for each locality. Filled symbols indicate $\delta^{18}O$-depleted rocks developed over 2.4 Ga high-Mg druzitic gabbro-norites, open symbols are depletions over Chupa gneiss, and half-filled symbol indicate a depletion happening in both 2.4 Ga meta-gabbro-norites and Chupa gneiss. B) Distribution of minimum $\delta^{18}O$ and δD values along the Belomorian Belt.

contemporaneous volcanics are interpreted to represent a plume type environment (Puchtel et al., 1997; Sharkov et al., 1997). Additionally, at 2.1 Ga, the Belomorian Belt experienced intrusion of small volume, Fe-rich, tholeiitic dikes, following local brittle deformations (Stepanov, 1981; Stepanova et al., 2003), and again these dikes suffered variable degrees of Svecofennian metamorphism, the intensity of which increases towards the Kola Peninsula.

### 1.2. $\delta^{18}O$ depleted rocks of the Belomorian Belt

First short reports on $\delta^{18}O$ depletion in Karelia appeared in 2007 and 2008 by three independent groups of Russian researchers (Krylov, 2008; Krylov and Glebovitsky, 2007; Ustinov et al., 2008; Visotskii et al., 2008) and dealt with three well-known localities of museum specimen quality corundum, kyanite, and garnet, all within 50 km from each other: Khitostrov, Varatskoye, and Mt. Dyadina (Fig. 1). These gemological localities were known to mineralogists and gem collectors since prospecting corundum-bearing rocks of Karelia in 1960–1970, and were investigated initially for the purpose of using the unique $\delta^{18}O$ values of corundum (ruby) minerals as a tool to fingerprint their origins (e.g. Giuliani et al., 2005). A weathering crust origin for the depleted values has been proposed by Krylov and Glebovitsky (2007), while Krylov (2008) and Visotskii et al. (2008) suggested that low-δ18O deep metamorphic fluids were involved, while Ustinov et al. (2008) suggested that meteoric fluids propagated into the zone of kyanite-grade regional metamorphism during Svekofennian 1.9 Ga orogeny.

Bindeman et al. (2010) argued against metamorphic origin to explain the depletion and investigated six samples from Khitostrov using single crystal O and H isotope analysis; these authors found 9‰ isotope heterogeneity (−25 to −16‰) between samples and within samples which they attributed to features associated with shallow-level hydrothermal alteration at high but variable water-rock ratios. U–Pb dating and in situ $\delta^{18}O$ determination within dated spots in zircons identified 2.8–2.55 Ga cores with normal-$\delta^{18}O$ igneous core values of 5 to 8‰, and −26‰, 1.9 Ga rims. Such record low-$\delta^{18}O$ values can only be explained by protolith alteration using synglacial waters, in which normal-$\delta^{18}O$ detrital zircons survived alteration but low-$\delta^{18}O$ oxygen was incorporated into other minerals and subsequently into zircon rims during the 1.9 Ga Svecofennian metamorphism.[1] Because the current paleogeographic knowledge suggests that Karelia was at low to mid latitudes between 2.5 and 1.8 Ga (Evans and Pisarevsky, 2008), and because there is a proposed glacial episode represented by Sariolian sedimentary sequences (Bekker, in press; Ojakangas et al., 2001), the oxygen isotope depletions in Karelia were tied together with the Slushball Earth glaciation episode at ca. 2.4 Ga (Bindeman et al., 2010).

In this paper, we report the discovery of seven new $^{18}O$-depleted localities and present our new results from geologic and isotopic mapping and petrological investigation of three previously identified, and better exposed localities (Khitostrov, Varatskoye and Mt. Dyadina). To understand the origin and determine the timing of isotopic depletion requires looking through the effects of 1.9 Ga Svecofennian metamorphism by relying on single crystal isotopic methods (e.g. Bindeman, 2008) to unravel the complex history of these rocks.

## 2. Methods

In this work we utilize mapping, thin section mineralogy, single crystal oxygen and hydrogen isotope analysis by laser fluorination, and by thermal combustion element analysis. Analytical details are provided in the Supplementary materials.

## 3. Results

### 3.1. New localities of $\delta^{18}O$ depleted rocks and their spatial distribution

In the search for low-$\delta^{18}O$ rocks we used the principle of analogy by investigating all known corundum-bearing localities across the Belomorian Belt, the majority of which occur in the Chupa complex; this approach proved fruitful and we identified ten localities with variably depleted oxygen isotopic values that now span 220 km along the Belomorian Belt (Fig. 1, Table A1, Appendix). Nine of them occur in the Chupa gneiss complex: Khitostrov, Mt. Dyadina, Varatskoye, Kulezhma, Plotina, Pulonga, Height 128, Lyagkomina, and Peruselka, and one locality (Mironova Guba) belongs to the Kovdozero gneiss complex closer to the Karelian craton (Serebryakov and Aristov, 2004). Studied localities differ dramatically in the level of $\delta^{18}O$ depletion (Fig. 1, Table A1). Four of them (Khitostrov, Varatskoye, Height 128, Plotina) have record low-$\delta^{18}O$ values for any rock on Earth (−7 to −27.3‰), significantly lower than the −3 to −10‰ $\delta^{18}O$ values measured in Dabie Shan and Kokchetav (Masago et al., 2003; Rumble and Yui, 1998; Zheng et al., 2004). It appears that the $\delta^{18}O$ depletion is more pronounced in the center of the 220 km-long zone along the Belomorian Belt. Geologic, geochronologic, and mineralogical similarities of all studied localities convincingly suggest that they formed at the same time and by similar processes (e.g. Serebryakov, 2004). The lowest $\delta^{18}O$ value we measured on Khitostrov (−26.9 to −27.3‰ garnets, corresponding to −27‰ rock, sample X425). We devoted most isotope sampling and most attention to this locality for the reasons outlined above: the lowest measured $\delta^{18}O$ rock give an upper bound on the $\delta^{18}O$ of meteoric water in a search for the lowest $\delta^{18}O$ rocks and estimating their extent (Figs. 2–4).

As $\delta^{18}O$-depleted rocks encompass hundreds of meters in each locality, their total volume is measured in cubic kilometers of rocks. Given the level of geological exposure of Karelia at 5%, and large distances between studied low-$\delta^{18}O$ localities covered by the Quaternary glacial deposits, it is conceivable that their number and total volume of remarkably $\delta^{18}O$-depleted rocks could be much larger, and goes beyond corundum-bearing lithologies. However, this would be difficult to recognize without the guiding principle of corundum presence by blind sampling, given high-amplitude $\delta^{18}O$ variations.

Our regional sampling of the Chupa gneiss itself indicated high-$\delta^{18}O$ values of +8 to +10‰, and rather similar $\delta^{18}O$ composition over large distances; earlier sampling and isotope analyses of 12 rocks spread across the Chupa gneiss by Salje et al. (1983) and Krylov (2008) also returned $\delta^{18}O$ values of ~+9‰ suggesting that 2.6 Ga gneiss is not $\delta^{18}O$ depleted and that $\delta^{18}O$ depletion postdates its formation.

In our attempt to expand the zone of low-$\delta^{18}O$ depletion, we have also analyzed corundum-bearing rocks from Kii Island in the southern end of the White Sea, 400 km to the south, where the Belomorian Belt project (Fig. 1), but obtained normal $\delta^{18}O$ values (ca 5.5–6‰, Table A1). Gem-quality corundum metasomatites from the late Archean Fiskenaesset deposit in SW Greenland, also returned normal $\delta^{18}O$ values.

In this work we rely on results of our 2010 fieldwork, regional geologic mapping of Miller and Milkevich (1995), Myskova et al. (2003), and local large scale mapping of gem localities performed by Serebryakov (2004) and Serebryakov and Aristov (2004) over several years of mineralogical investigations.

[1] Due to zircon's refractory nature, hydrothermal alternation does not change the U–Pb age nor the original $\delta^{18}O$ values of the zircons as has being demonstrated in hydrothermal systems (e.g. Skaergaard; Bindeman et al., 2008). Shallow hydrothermal alternation in Karelia severely and heterogeneously depleted $\delta^{18}O$ values of host rock, likely turning them into clays, and bringing them down to -27‰, but zircons retained their original +5 to +7‰ igneous or detrital cores; on high temperature recrystallization with migmatization caused exteriors of zircon to recrystallize, forming metamorphic 1.87 Ga, Low-$\delta^{18}O$ rim, in equilibrium with local metamorphic assemblage. Based on the age-$\delta^{18}O$ relationship (Bindeman et al., 2010), the age of hydrothermal alteration, Chupa gneiss near surface residence, and whole-rock $\delta^{18}O$ depletion at large water-rock ratios is permissible between 2.5 and 1.9 Ga.

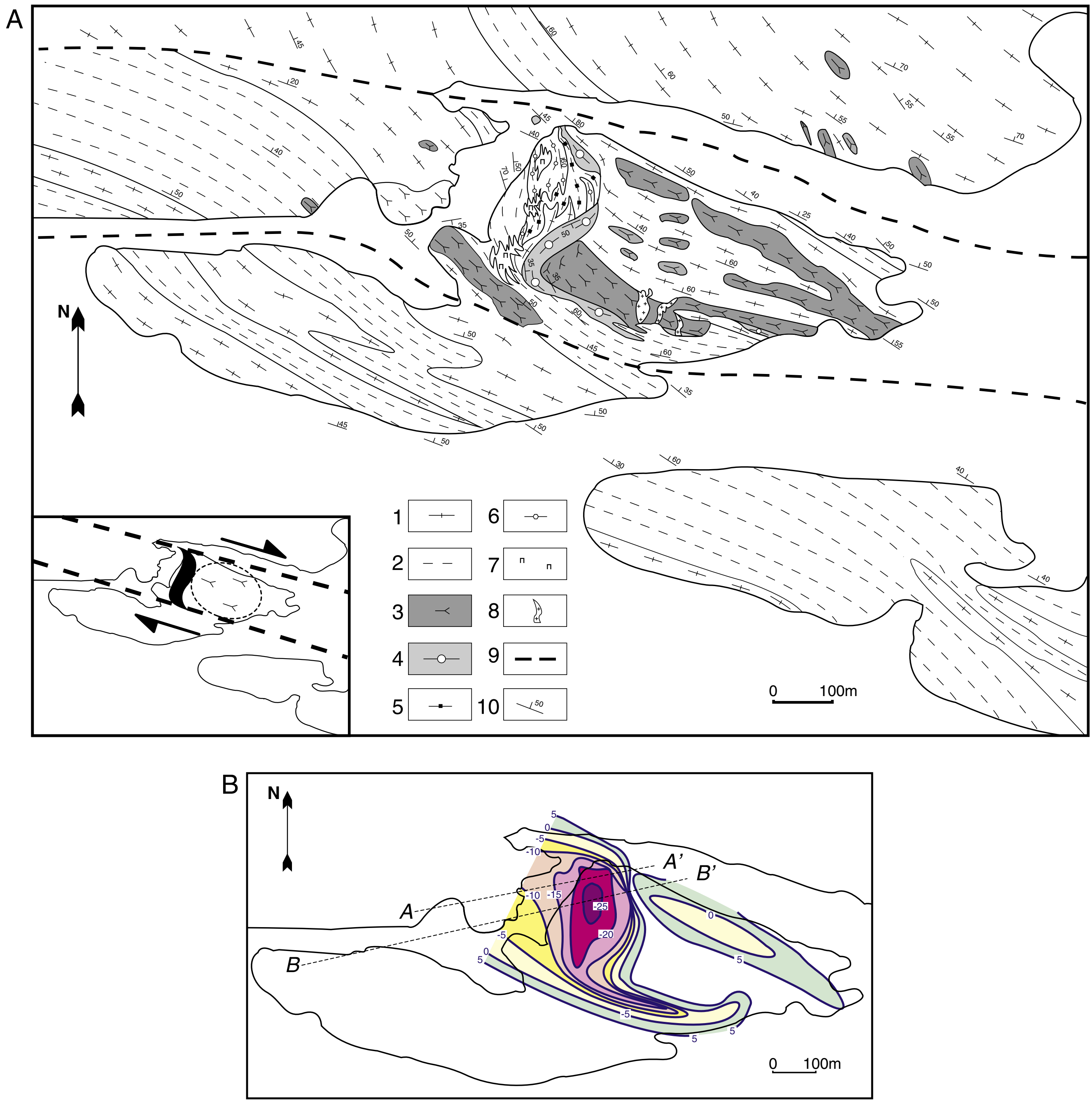


**Fig. 2.** Geologic map of Khitostrov locality (A, modified after Serebryakov, 2004), with isotope contour map (B), see Fig. A2 for sampling localities and Table A1 for $\delta^{18}O$ values. A) rock distribution: 1—Bi-Gt Chupa gneiss; 2—Ky-Bi-Gt Chupa gneiss (near the contact with Crn rocks it lacks Qz and has large Ky); 3—Fe-gabbro and gabbro-amphibolite; 4—migmatized Gt-amphibolites; 5—St-Gt-Bi-Ts-Pl-rock with St-Pl pseudomorphs over Ky; 6—Crn-St-Grt-Ged-Prg-Pl-rock with Crn-St-Pl pseudomorphs over Ky (near contacts with 5) and with large idiomorphic crystals of Crn (in central part, with maximum $\delta^{18}O$ depletion); 7—plagioclasites; 8—pegmatites; 9—faults; 10—strike and dip; Inset on the bottom right shows regional geologic features, with two strike-slip faults and S-shaped flexture. B) Isotope contour lines which are superimposed on the map showing concentric bulls-eye pattern, and position of profiles A–A' and B–B', see Fig. 4A,B. Mineral abbreviations used on this figure and throughout the paper, given alphabetically: Amph, Hb—amphibole, Ant—antophillite, Bi—biotite, Cam—Ca-amphibole; Chl—chlorite, Crn—corundum, Ged—gedrite amphibole, Gt—garnet, Ky—kyanite, Mgn—magnesite, Oam—orthoamphibole, Opx—orthopyroxene, Pl—plagioclase, Prg—pargasitic amphibole, Px—pyroxene, Ru—rutile, Qz—quartz, Sp—spinel, Spr—sapphirine, Ts—Tschermakitic pyroxene; St—staurolite, Zo—zoisite, Zrc—zircon.

### *3.2. Description of $\delta^{18}O$, $\delta D$ depleted localities*

In our isotope mapping we predominantly used refractory minerals such as garnet, corundum, kyanite and amphibole and the $\delta^{18}O$ values in minerals were used to constrain bulk rock values. Retrogression modeling, using fast grain-boundary diffusion models (Eiler et al., 1994; Peck and Valley, 2000) demonstrates that garnet, corundum, kyanite, and amphibole do not exchange oxygen at any rate of cooling, reflecting peak-metamorphic $\delta^{18}O$ values; while rutile, plagioclase, quartz and biotite retrogress by less than one permil even at slow cooling rates (Fig. A1, Appendix).

In total we report 209 new $\delta^{18}O$, and 35 new $\delta D$ analyses for ten localities, and discuss them in conjunction with 105 ($\delta^{18}O$) and 35($\delta D$) analyses of Khitostrov from Bindeman et al. (2010), and correlate them in space and between different rock types within each locality, enabling us to draw isotope contour maps and isotope profiles. Analyses are given in Tables A1–A2 in Appendix, and below we provide description for studied localities, following mineral abbreviations as in Fig. 2.

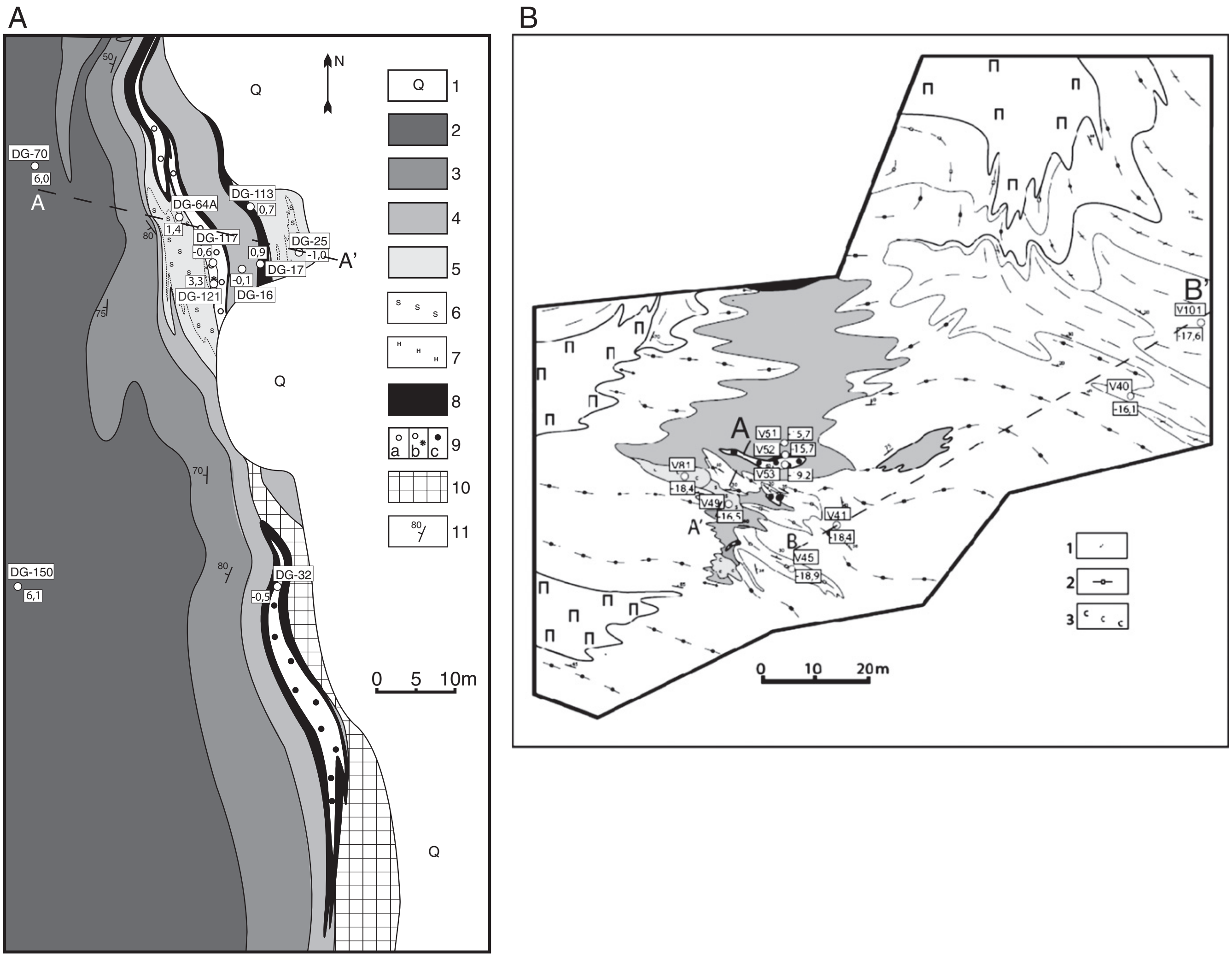


**Fig. 3.** Geologic map of the Mt Dyadina (A) and Varatskoye (B) corundum deposits (modified after Serebryakov, 2004) with sampling localities and $\delta^{18}O$ values. A) Mt Dyadina, key to rock types: 1—Quaternary deposits; 2—gabbro-norites; 3—fine-grained amphibolites with or without garnet; 4—coarse-grained Grt-Hbl(±Qtz-Pl) rocks; 5—coarse-grained Ky-Gr-Ts rocks; 6—same as 5 but with Crn and with St-Pl symplectite over Ky; 7—Hb-Spl-Ts rocks; 8—Ky-Hbl-Oam(±Grt) rocks; 9—rocks with giant garnets: a—Gedritites (Grt±Hbl-St-Ky-Crn-Bt); b—Grt-Mgh-Spr-Ged rocks; c—Grt-Chl±Ant, Hbl, St, Crn rocks; 10—Qz-Zoisite rocks; 11—shistosity. B) Varatskoye, Zoning of Crn rocks in Ky gneisses: 1—Ky-Qtz-Bt-Grt-Ts-Pl rock; 2—Crn-St-Bt-Ts-Pl-rocks with Crn-St-Pl pseudomorphs over Ky and large idiomorphic crystals of Crn. Zoning in rocks over gabbro-norites: 3—Crn-Grt-Cam-rocks (±Hb); see Figs. 2 and 3A for other symbols.

Khitostrov. Oxygen isotope depletions characterize an area of 500×300 m and the distribution of O isotopes in space (Fig. 2) reveals that low $\delta^{18}O$ values broadly correspond to the occurrence of the corundum-bearing rocks, but depletion affects host gneiss and Fe-amphibolites as well. We discover that there is a concentric distribution of $\delta^{18}O$ in space (Figs. 2B and Fig 4A–B). The most depleted rocks are located in the 'bull's-eye' center of the corundum deposit; a separate bulls-eye with a moderately low-$\delta^{18}O$ zone exists in the gneiss to the east. Oxygen depletion increases towards the rocks with lower SiO2 and higher Al/Si, Zr/Si, and Ca/Si ratios (Table A2, Appendix).

The lowest whole-rock $\delta^{18}O$ value of −27‰ (X425) that we were able to identify by isotope mapping is 2–3‰ lower than previously measured, and the rock is an ordinary looking, medium-grained Pl-Cam-Ged-Gt-St-Crn-Rt±Bi assemblage (samples X423 to 426, and K2 and K3 of Bindeman et al. (2010), see Fig. 4, Figs. A3a and 4B, Appendix). These rocks are in the middle and upper portion of the bull's-eye $\delta^{18}O$ depleted zone. The most $\delta^{18}O$-depleted Pl-Cam-Ged-Gt-St-Crn-Ru rock is locally invaded and substituted by higher $\delta^{18}O$ plagioclasite veins (sample X112, $\delta^{18}O = -8.8$‰, Fig. A3); it appears that this process leads to the formation of large crystals (up to several centimeters) of ruby corundum, on the contact between the leucosome and melanosome. This process produces leucosome–melanosome alteration with high-amplitude $\delta^{18}O$ variations in between, on an outcrop to a hand specimen-scale (Fig. A3). We interpret this process to complicate the $\delta^{18}O$ variations in addition to the proposed high amplitude $\delta^{18}O$ variations due to variable water–rock ratios in the protolith during hydrothermal alteration, (cf. Bindeman et al., 2010). Indeed, preservation of pre-metamorphic heterogeneous $\delta^{18}O$ values attributed to the protolith are known even in granulite facies rocks (Anderson, 1967; Valley and O'Neil, 1984). In Khitostrov, both isotopic variations and synmetamorphic plagioclasite replacement may be responsible for isotope disequilibria in minerals and for $\delta^{18}O$ zoning within single crystals of large corundum. Furthermore, oxygen isotopic investigation of 1.9 Ga zircon rims by ion microprobe reported by Bindeman et al. (2010), has resulted in a range of $\delta^{18}O$ values from −26.2 to −23.9‰. This range may also reflect site-specific recrystallization of these zircons under the influence of higher $\delta^{18}O$ plagioclasite, thus elevating the initially very low $\delta^{18}O$ value of −26.2‰. Notice that the lowest-$\delta^{18}O$ zircon rim value of −26.2‰ would be in equilibrium with the lowest $\delta^{18}O$ garnet values of this study.

Other higher $\delta^{18}O$ rocks that are observed to structurally and texturally postdate metamorphic formation of the high-Al, lowest $\delta^{18}O$ rocks are muscovite-plagioclase-quartz metasomatites (sample

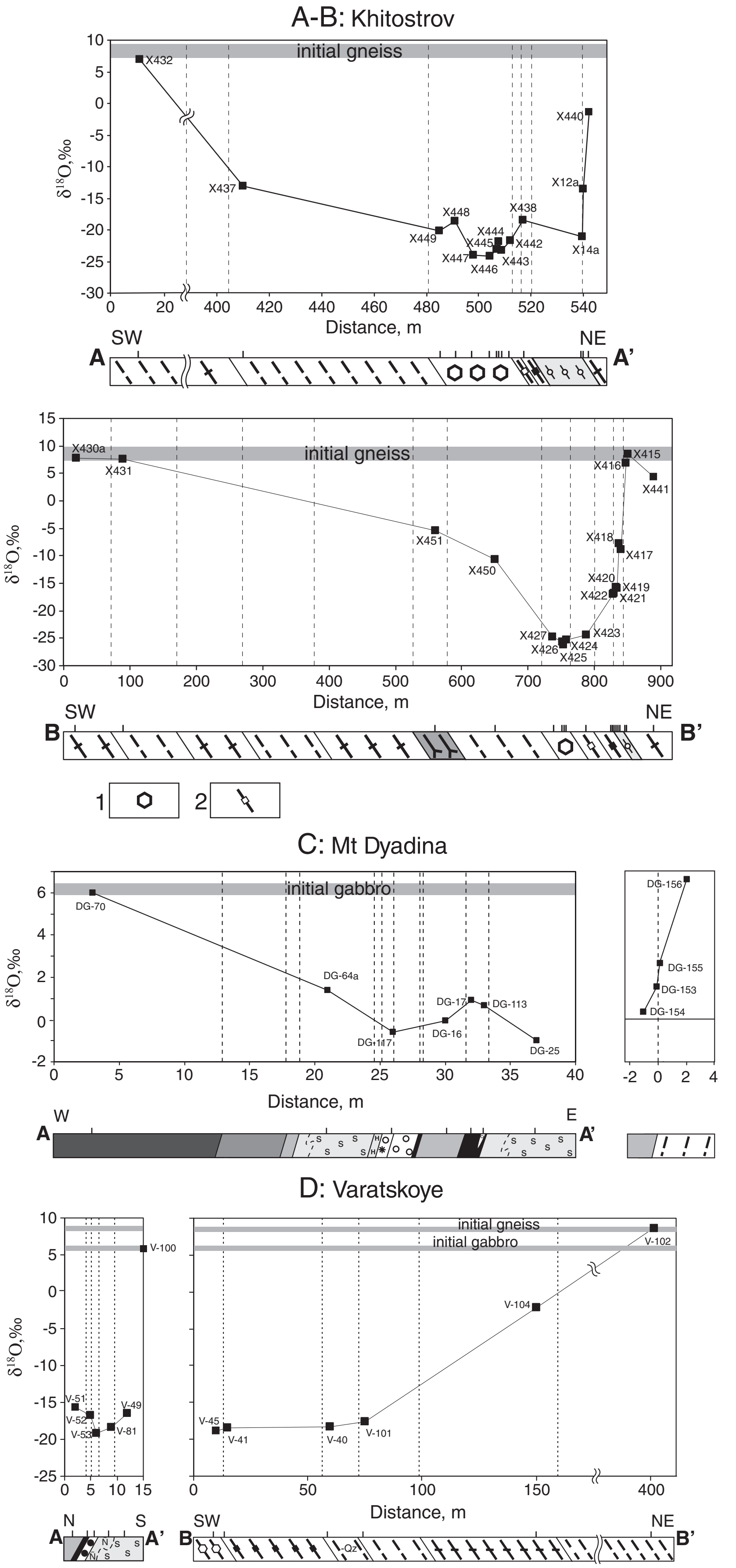


**Fig. 4.** Isotope profiles and rock types across lines shown in Figs. 2 and 3, sample numbers and $\delta^{18}$OWR values are from Table A1. A–B) Khitostrov. Crn-St-Gt-Ged-Prg-Pl-rock: 1—with large idiomorphic crystals of Crn, 2—with Crn-St-Pl pseudomorphs over Ky; C) Mt. Dyadina and D) Varatskoye. See Fig. 2a for symbols of rock types.

X428, with higher $\delta^{18}O = -4.6‰$), and later stage pegmatites (X401, $\delta^{18}O = +4.4‰$). Due to synmetamorphic transformation, the age and the original compositional characteristics of the mafic rocks on the island are less clear, pending dating; The nearest druzite body (X458) 3 km to the south is normal-igneous $\delta^{18}O$ of +5.5‰.

Mt Dyadina. Rocks depleted in $\delta^{18}O$ are exposed over the 400×40 m area on the edge of the druzitic gabbro-norite body, close to its unexposed contact with the Chupa gneiss. Structurally, the $\delta^{18}O$-depleted rocks form en-echelon lenses with cores made of rocks with giant (up to 30 cm) garnets inside of gedrite or chlorite matrix (Table A1, Fig. 3A, Fig. A3e, Appendix) This $\delta^{18}O$-depletion characterizes a variety of high-Al rock types with coarse-grained to giant-grained minerals, forming the following sequence from gabbro-norite to rocks with giant garnets (see Fig. A3d, and Table A2 in Appendix for chemical analyses): unaltered gabbro-norite (Pl-Cpx-Opx ± Gt, $\delta^{18}O = 6‰$) – amphibolite (Gt-Cam-Plag) – coarse-grained Gt-Cam rock ($\delta^{18}O = -0.1‰$), Oam-Cam ± Ky schist ($\delta^{18}O = 0.9‰$), giant garnet–gedrite schist (Gt-Ged-Crn, Garnet −0.6‰ in isotopic disequilibrium with Ged +2.1‰ and corundum +0.5‰). Coarse-grained garnet–gedrite schist is substituted by chlorite and antophillite but large garnet crystals preserve their $\delta^{18}O$ value of −0.5‰.

In other areas coarse-grained Gt-Cam rock ($\delta^{18}O = 0‰$) is substituted by Cam-Gt-Ky, followed by Cam-Gt-St ($\delta^{18}O = -1‰$), then by Cam-Crn ($\delta^{18}O = 1.4‰$), then by Cam-Spl-Hgb assemblages. At the same time, Gedrite-bearing rocks contain gedrite–sapphirine assemblages ($\delta^{18}O = 3.3‰$) with up to 20% of late stage, higher-$\delta^{18}O$, disequilibrium magnesite ($\delta^{18}O = 10.4‰$, $\delta^{13}C = -7.4‰$).

The $\delta^{18}O$ variations across sharp, 1 m thick metagabbro-norite-Ky-gneiss contact zone, trenched 400 m away (Table 1, Fig. 4A), demonstrates that the large garnets were developed inside the endocontact zone, and the quartz-richer gneiss in the exocontact. Both gneiss and gabbro–amphibolite at the contact are lower in $\delta^{18}O$ (0.5–1.6‰), but are normal in $\delta^{18}O$ only meters away.

The chemical change that accompanies the mineralogical zoning and $\delta^{18}O$ depletion is reflected in wide ranges of $SiO_2$ and $Al_2O_3$ concentrations from 52% and 12% in gabbro to 38% and 26% in Mgn-Spl-Ged schist Serebryakov (2004) and Serebryakov et al. (2007) Mgn-Sp respectively (Table A2, Appendix). Corundum-bearing rocks are significantly enriched in 4+ and 5+ valence elements, richer in Mg and poorer in alkalies.

Varatskoye. The rock types that are found at Varatskoye are exposed over 250×150 m area and include both the original Chupa gneiss (like at Khitostrov) and amphibolitized and metamorphosed druzitic gabbro-norites, similar to Mt Dyadina (Fig. 3B and 4D). The gabbro-norites are strongly metamorphozed and are represented by nearly monomineralic amphibolite with (V51, $\delta^{18}O = -15.7‰$, $\delta D = -226‰$). This mafic rock is chemically similar to the normal-$\delta^{18}O$ druzite gabbro-norite that is exposed two kilometers away (sample V100).

A series of mineral assemblages are developed within the mafic rocks and the generalized profiles are presented on Fig. 4D profiles A–A': a zone with two amphiboles ($\delta^{18}O = -15.7‰$, $\delta D = -224‰$), then 0.5–2 m thick zones with kyanite and St-Pl substituting Ky ($\delta^{18}O = -16.5‰$, $\delta D = -218‰$) and corundum ($\delta^{18}O = -18.4‰$, $\delta D = -228‰$), and finally the zone with giant garnets ($\delta^{18}O = -19.2‰$), that are texturally substituted by retrogressed assemblages of Ged ± Cam + Sp, then Chl + Bi, gedrites ($\delta^{18}O = -8‰$) are in $\delta^{18}O$ disequilibrium with the garnet. It is interesting to note that both the sequence of mineral assemblages and the overall decrease in $\delta^{18}O$ toward more Al-rich core at Varatskoye, is similar to the change described above at Mt Dyadina, although the $\delta^{18}O$ values are significantly lower.

The mineralogical change over the silicic Chupa gneiss nearby (Fig. 4D profiles B–B′) is as follows: the original Qz-Ky gneiss ($\delta^{18}O = 9‰$), a gneiss with less quartz and +Cam, 150 m away from the mafic body ($\delta^{18}O = -2.2‰$), Ky-Gt-Bi schist without Qz 50 m away ($\delta^{18}O = -17.6‰$), Pl-Bi-Gt-Cam-St rock with St-Pl substituting Ky and Pl-Cam-Bi-St-Crn ± Ap rock 1–10 m in width, with St-Pl substituting Ky ($\delta^{18}O = -19‰$; $\delta D = -235‰$) closer to the mafic body. This type of mineralogical zoning, lowering of $\delta^{18}O$ values toward the coarse-grained zone with corundum, and progressive increase in Al/Si ratio, is reminiscent of that in Khitoostrov, described above. The difference is that at Varatskoye, all rocks are more uniformly lowered in $\delta^{18}O$ and $\delta D$. The $\delta D$ reach the lowest values of −224 to −235‰, measured in dominant, coarse-grained, rock-forming amphibole with 2 wt.% water, in assemblage with staurolite (−221‰). Such values are the lowest $\delta D$ values reported for silicate rocks on Earth to our knowledge. They plot on the 'wrong' side of the meteoric water line on $\delta D$-$\delta^{18}O$ diagram (Fig. 5), which can be explained by water loss (higher in $\delta D$) during metamorphic

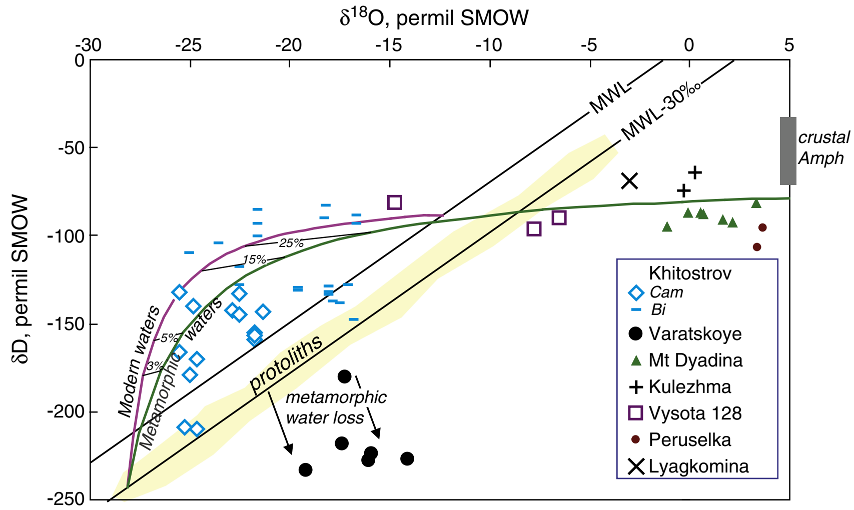


**Fig. 5.** $\delta D$ vs $\delta^{18}O$ diagram plotting data for biotites and amphiboles from individual crystal clusters. Notice that studied rocks are significantly lower in $\delta D$ and $\delta^{18}O$ than any typical crustal and mantle amphibole (>5‰ $\delta^{18}O$ and ≥– 80‰ $\delta D$). The represented range suggests depleted but highly variable in $\delta D$ and $\delta^{18}O$ protoliths for each indicated locality (shown in yellow), explained by differing water-rock ratios during Paleoproterozoic hydrothermal alteration. Data points from monoamphibolitic or amphibole-dominant assemblages from Varatskoye with highly negative $\delta D$ values are best explained by the effects of metamorphic water loss, data points from Khitostrov are best explained by alteration of an initially very depleted protolith (ca −28‰ $\delta^{18}O$) by higher in $\delta^{18}O$ and $\delta D$ fluids of either deep metamorphic ($\delta^{18}O = 5‰$, $\delta D = -80‰$), or modern surface waters ($\delta^{18}O = -11‰$, $\delta D = -90‰$). Data points from other localities can also be explained by alteration by a metamorphic fluids upon retrogression. MWL is meteoric water line, MWL-30‰ is offset by 30‰ The $\delta D$ values in the primary protolithic micas and amphiboles were offset by −30‰ $\delta D$ to account for for water-hydrous mineral fractionation at metamorphic temperature of 600 ± 100 °C that correspond to observed kyanite facies metamorphic grade.

devolatization. Ion microbrobe investigation of zircons found similar results to those found at Khitostrov: normal $\delta^{18}O$ 2.8–2.6 Ga cores, and Svekofennian-age, −20‰ rim.

Kulezhma. The distribution of lithologies at Kulezhma is very similar to that at Mt. Dyadina: coarse grained, giant garnet and large kyanite-bearing rocks are found at the edge of small druzitic gabbro-norites body intruded into Chupa gneiss. The outcrop is 100×15 m and it has the same rock types: least metamorphosed gabbro-norite (Opx-Cpx-Plag), substituted by Gt-amphibolites, then by Oam-Cam-Gt-Ky schists, then by Cam-Ky rock with staurolite-plagioclase symplectites over kyanite and minor corundum, then by zones with giant garnets. Oxygen isotopic values of garnets in the center zones are also similar to Mt Dyadina and range from −0.3 to +0.3‰ (Table A1).

Height 128. Geologic position and mineralogical changes in this 100×40 m locality are reminiscent of Varatskoye, as high-Al corundum bearing rocks are developed over the druzitic meta-gabbro and Chupa gneiss in close vicinity of one other, and blocks of fresh druzitic gabbro-norite occur nearby without clear visible contact with the coarse grained high-Al amphibolites and metagneiss. Oxygen isotopic values measured in three rocks range from −6 to −14‰ (sample KV-4), but the most $\delta^{18}O$-depleted value characterizes the Ky-gneiss, not the corundum-bearing rocks, although in close (20 m) proximity to them. Zircon rims by ion microprobe analysis in sample KV-10 are in equilibrium with the matrix at −11‰, while cores have normal igneous $\delta^{18}O$ values of 5 to 7‰.

Other localities. At Lyagkomina and Plotina, coarse grained rocks with plagioclase + staurolite and plagioclase + corundum symplectite are developed over kyanite gneiss; the $\delta^{18}O$ values are as low as −3‰, and zircon rims down to −5‰. The types of rocks and mineral assemblages are very similar to that of Khitostrov. At Peruselka and Pulonga, the corundum-bearing coarse-grained amphibolitic rocks developed over metamorphosed mafic intrusions, very similar to the Mt. Dyadina locality. At these two localities $\delta^{18}O$ values are depleted down to 1 to 3‰, with δD values in amphibole down to −107‰, the third lowest value among studied rocks. At Mironova Guba, isotope depletions characterize the Crn-bearing rocks at the edge of a similar amphibolitic gabbro body which is intruded into Kotozero suite gneiss (Lobach-Zhuchenko et al., 1995), the only $\delta^{18}O$-depleted locality in our dataset outside of the Chupa complex.

### *3.3. General mineralogical and chemical trends in the $^{18}O$ depleted localities*

As described above, the ten localities of $^{18}O$-depleted rocks are developed over two protoliths: high-Al Chupa or Kotozero gneisses and metagabbroic druzite bodies, and in some cases, near the contact between the two. The druzitic bodies represent a Karelia-wide stage of plume-related magmatism of short duration at 2.45–2.4 Ga (Amelin et al., 1995; Bibikova et al., 2004; Puchtel et al., 1997). The main chemical and mineralogical trends in these localities include the progressive increase in Al and decrease in Si toward the center, with variable behavior of other components. Compiled representative analyses for major and trace elements in the Chupa gneiss, gabbro-noritic bodies, and the low-$\delta^{18}O$, high-Al rocks within them (Table A2, Appendix) demonstrate a decrease in $SiO_2$ (accompanied by the diminution and disappearance of modal quartz) and an increase in Al, REE, and 4+ and 5+ valent HFSE elements such as Zr, Ti, P, and Nb by a factor of 1.5 to 3 toward the center of the bull's eye zones. Estimates based on increasing concentration of insoluble element Zr call for 30–60% of the original parental rocks to be dissolved. Similar estimates could be obtained using Ti. This fluid flushing and dissolution have affected other elements in different proportions causing wide variations in their concentrations and ratios (e.g. K/Na, Rb/Na, Sr/Ba, Table A2).

In general, this chemical change is accompanied by the following mineralogical change from the host gneiss to the core of corundum bodies:

Qtz–Pl–Bt–Grt–Ky → Pl–Bt–Grt–Ky → Pl–Cam–Gt–St ± Bt → Pl–Cam–(Na–Ged)–Gt–St–Crn ± Bt

In the latter two assemblages, kyanite is replaced by pseudomorphs of St-Pl and Crn-Pl symplectites, respectively (Figs. A3b and A4c,d, Appendix).

In metagabbroic corundum-bearing bodies, the sequence is more complicated and can be classified into two paths:

1) Pl–Opx–Cpx (gabbro–norite) → Pl–Cam–Gt ± Qtz → Cam–Gt → Cam-Oam ± Ky,Grt → Ged-Ky ± Gt → Ged–Gt ± Crn,Cam
2) Pl-Opx-Cpx (gabbro-norite) → Pl-Cam-Grt ± Qz → Cam-Grt → Cam-Ky ± Grt → Cam-Crn ± Gt, (St + Pl) → Cam-Spl-Hgb → Ged-Spr-Mgn-Grt (the later two assemblages occur only on Mt Dyadina). Additionally, a retrogressed assemblages of Chl–Gt–Ant–Cam ± Bi often substitute the giant garnet cores.

### *3.4. Hydrogen isotopes in $\delta^{18}O$ depleted rocks*

Hydrogen isotope analyses were performed on single and bulk biotite and amphibole crystals extracted from crystal clusters (new data Table A1, and those from Bindeman et al., 2010). In the two most $^{18}O$ depleted localities, Khitostrov and Varatskoye, the δD values are lowest for terrestrial rocks: down to −212‰ and −235‰, respectively. Amphiboles collectively have lower δD values than biotites, and maintain equilibrium $\delta^{18}O$ fractionations with other minerals, while biotites in half of the samples from Khitostrov appear to be secondarily hydrated by heavier hydrogen from secondary or modern waters.

When plotted on $\delta^{18}O$-δD diagram (Fig. 5), amphiboles and biotite display significant ranges that can be explained by two processes:

1) retrogressive exchange of initially ultra-low (ca −24 to −30‰ $\delta^{18}O$, −170 to −250‰ δD) protoliths with a variety of younger and higher in $\delta^{18}O$ and δD waters of either deep magmatic–metamorphic, or surface-derived, meteoric origin. The lowest $\delta^{18}O$ and δD hydrous minerals support a −26 to −30‰ $\delta^{18}O$ protolith as a starting point.
2) Metamorphic devolatilization is the natural process capable of explaining amphibole-dominant samples plotting to the right of the meteoric water line (mostly from Varatskoye), as dictated by the sense of isotope partitioning (loss of heavier δD vapor), and as is observed in contact aureols (e.g. Ripley et al., 1992).

It is still remarkable that in these complex polymetamorphic rocks, a significant proportion of the initial Paleoproterozoic ultra-depleted meteoric hydrogen is still present, given the high susceptibility of hydrogen to get elevated by a variety of processes. We estimate that up to 75–99% of the original hydrogen is preserved (Fig. 5).

## 4. Discussion

### *4.1. The glacial source for low $\delta^{18}O$ rocks and the likely $\delta^{18}O$ values of waters*

We interpret the remarkably low-$\delta^{18}O$ and δD rock values as evidence of alteration by glacial meltwaters in cold climate conditions. Based on terrestrial $\Delta^{17}O = 0$ in these rocks (Bindeman et al., 2010), we discount extraterrestrial (e.g. cometary) origin of the Karelian depletions.

We take the minimum measured $\delta^{18}O$ rock value of −27‰ as evidence for the maximum $\delta^{18}O$ values of altering waters. This is because at hydrothermal temperatures of >350 °C, $\Delta^{18}O$(rock–water) fractionations are 0 ± 1‰, and at lower temperatures $\Delta^{18}O$(rock–water) fractionations are higher (Criss and Taylor, 1986), requiring even lower-$\delta^{18}O$ altering waters. Two additional reasons would support a meteoric water value lower than −27‰. As discussed in the Introduction, during hydrothermal alteration, water–rock isotopic exchange is rarely 100% and rarely brings rocks to $\delta^{18}O$ values of unshifted altering waters (e.g., Taylor and Sheppard, 1986). Second, based on the present investigation, we argue that $\delta^{18}O$ values recorded by rocks might also have been raised by synmetamorphic fluids during the Svecofennian metamorphism. We surmise that the circulating meteoric waters could have been ~10 permil lower than −27‰, (by analogy with hydrothermally-altered rocks in modern hydrothermal systems worldwide, see above) and below we discuss climate implications of −27 to −35‰ meteoric waters.

In the modern world, waters that are ≤25‰ are only found in glaciated areas of Greenland and Antarctica (www.waterisotopes.org). In this regard, it is highly likely that hydrothermal alteration of the Chupa and Kotozero gneisses and 2.4 Ga druzitic gabbro bodies was achieved by glacial meltwaters (Fig. 6). Thus, we envision the position of the Belomorian rift zone, and Karelia in general, under a continent-wide (at least 220 km-long) ice cap, during a time of very cold climate conditions, corresponding to −18 to −35 °C mean annual temperatures, by analogy with modern or Pleistocene glacial worlds (Fig. 7).

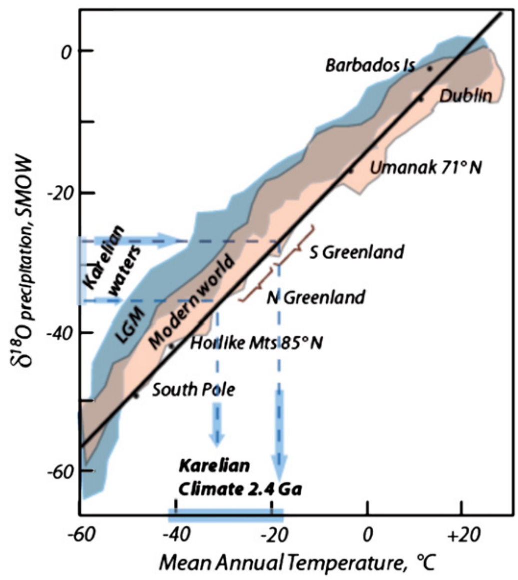


**Fig. 7.** Correlation of mean annual temperatures with $\delta^{18}O$ values of precipitation showing −18º to ≤35 º C temperatures for −27 to −35‰ meteoric waters. Fields labeled Modern world is modern precipitation data compiled by Jouzel et al. (1994), while field labeled LGM (Last Glacial Maximium) represent modeling result based on a circulation model of Jouzel et al. (1994). Thick line and geographic locations is based on global fit line of modern precipitation after (Dansgaard, 1964).

### 4.2. Summary of geological and isotopic observations

The following observations can be made for studied localities.

- The localities with depletion of $\delta^{18}O$ and δD are found in or near the edges of the 2.4 Ga amphibolitized gabbro-noritic bodies, 2.6 Ga Chupa gneiss, or near the contact of the two.
- The known lateral extent of depletions in $\delta^{18}O$-depleted rocks is hundreds of meters.
- In each of the localities, the $\delta^{18}O$ values form concentric, bull's-eye patterns (often elongated by shear zones) with the maximum $\delta^{18}O$ depletion in the center; this coincides with desilication trend; the center is represented by corundum-bearing, Qtz-free rocks, richer in Zr and Ti, zircon and rutile; in all localities, assemblages are coarse-grained to giant-grained. At the same time, isotope depletions affect rocks of all types and the boundaries of $\delta^{18}O$ depletions extend tens of meters into ordinary-looking parental Chupa gneiss or gabbro-norites (Fig. 2).
- Gradients in $\delta^{18}O$ could be very steep and sometimes exhibit tens of permil variations on a meter scale; isotope disequilibria on the order of several permil characterize hand specimens, and in some cases, individual large minerals (Bindeman et al., 2010).
- Hydrogen isotopic values are the lowest reported for terrestrial rocks and require that the original low δD protolith was affected by volatilization and the loss of heavier δD water, or perhaps alteration by higher δD, higher $\delta^{18}O$ secondary magmatic, metamorphic, or surface waters.

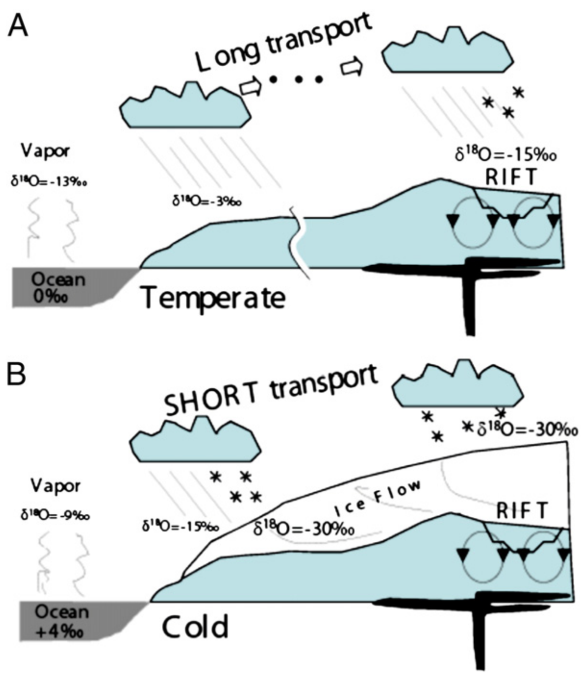


**Fig. 6.** Conceptual model of rifting under ice and $\delta^{18}O$ vapor distillation as a function of climate for different paleogeographic conditions. (A) modern climate conditions and isotope distillation into a medium-large size continent (such as N. America or Eurasia) with an intracontinental rift zone that leads to −10 to −15‰ annually-averaged $\delta^{18}O$ groundwater in higher-latitude, intracontinental rift zones (e.g. water in Lake Baikal rift is −16.5‰, Wickham et al., 1996), (B) Greenland-like or a Slushball Earth environment with low-$\delta^{18}O$ ice reaching shores. The $\delta^{18}O$ value of seawater is elevated above that during the last ice age because of the amount of ice frozen on continents is greater; colder climate leads to greater $\delta^{18}O$ water-vapor isotope fractionation and ice flow from higher altitude leads to low-$\delta^{18}O$ glacial meltwaters affecting subglacial rifts. If significant amounts of sea-ice is present, it may somewhat compensate for seawater enrichment ($\Delta^{18}O$ ice-water = 3‰, O'Neil, 1968) values of seawater; most depleted $\delta^{18}O$ values are possible to achieve in this case. Isotopic values for waters and isotope fractionations are quoted for reference only and could differ by a few‰ depending on particular paleogeography-climate conditions.

### 4.3. Chemical change and $\delta^{18}O$ depletion: hydrothermal vs. metamorphic

The apparent correlation of $\delta^{18}O$ decrease toward the center of desilicified zones lead us to discuss two reasons for the presence of the lowest $\delta^{18}O$, coarsest-grained, high-Al cores with corundum (metasilicic) or giant garnets (mafic) lithologies, that are most enriched in insoluble elements Al, Zr, Ti, REE, and accessory minerals, rutile, zircon, orthite (Figs. A3–A4, Table A2, Appendix).

First, hydrothermal alteration and dissolution of the protolith near the surface at 2.4 Ga depleted these rocks with respect to $\delta^{18}O$, leading to a bull's-eye alteration pattern, common in many shallow meteoric-hydrothermal systems worldwide (e.g. Taylor and Sheppard, 1986). Enrichment in Al, Zr and Ti occurred through mass loss upon rock dissolution. Dissolution of the starting Chupa gneiss in pH-neutral meteoric water hydrothermal solution at 200 °C and 0.1 kbar using the CHILLER program (Reed, 1983; Spicher and Reed, 1989) produces the required trend of Si and Al with water/rock ratios of >400. (Table A2, Appendix).

Second, because now-metamorphic rocks exhibit coarse to giant-grained textures, show psuedomorphic, symplectitic and reactive mineral relations, and because the distribution of these patterns is interpreted to have been controlled by (or coeval with) the 1.9 Ga shear zone (Fig. 2A), we agree that some chemical mass redistribution happened during the 1.9 Ga Svecofennian metamorphism. The second author of this publication (NS) prefers that most of the chemical changes (including Al/Si and other ratios) happened synmetamorphically, in the focused fluid flow that was controlled by the transtension duplex in the shear zone (including sigmoidal fold and en echelon pegmatite veins in metagabbro boudin) that we mapped (Fig. 2, Serebryakov, 2004; Serebryakov and Rusinov, 2004).

In either interpretation, these synmetamorphic fluids were undoubtedly derived from the same ultra-low-$\delta^{18}O$ premetamorphic protolith, just from its deeper parts, and must not have traveled long distances through other rock types, because any such fluid percolation would have erased their low-$\delta^{18}O$ signatures. An interesting follow-up to this interpretation is that it offers the possibility that the unexposed source protolith for these fluids could have been even lower in $\delta^{18}O$ than what its fluids imparted on the exposed rocks.[2] During the Svecofennian metamorphism, these fluids caused zircon to recrystallize, exchanging oxygen with nearby minerals, yielding −26‰ equilibrium zircon rims (Bindeman et al., 2010).

Our interpretation contrasts sharply to statements by some investigators that syn-metamorphic low-$\delta^{18}O$ Svecofennian fluids were external to the protolith, or that they were brought to the 20–25 km metamorphic depths from the deep crust or mantle, or from above along fault zones. Hydrologically, it would be impossible to get −20 to −30‰ surface fluid at the inferred 7 kbar kyanite-grade Svecofennian metamorphism and keep it isotopically-unshifted (i.e. ca at ≤26‰) to exchange oxygen with large volumes (ten to hundred cubic kilometers) of the initially high-$\delta^{18}O$ Chupa gneiss. Also, regional metamorphic fluids at 1.9 Ga were clearly normal to high in $\delta^{18}O$[2], as is sampled by pegmatites, and Svecofennian metasomatites without corundum in Khizovara and Vincha localities (Table A1).

Given that the protolith for the pre-1.9 Ga low-$\delta^{18}O$ rocks could have been even lower in $\delta^{18}O$ than is currently observed or exposed, and because it could have been locally affected by higher $\delta^{18}O$ Svecofennian fluids, in situ investigation of $\delta^{18}O$ in the refractory mineral zircon, that is not affected by these fluids, will be provided in our companion paper.

### 4.4. Type of hydrothermal alteration

If oxygen isotopic depletions were to be explained by the same process that created their high-Al nature, and caused enrichment in Zr and Ti, then a shallow-level process with a large fluid/rock ratio that removes silica relative to Al, Ti and Zr is required. Chemical and isotopic changes around contact aureoles of Phanerozoic intrusions vary greatly (e.g. argillitic, propylitic, greisen, Na and K-metasomatic and many others) and is the function of the emplacement depths, chemistry of fluids, types of waters, permeabilities, and oxidation state (Rye et al., 1991). The observed chemical change toward high-Al rocks in the center of the bull's-eye pattern, may be similar to modern analogs of advanced hydrothermal alteration (Rye, 1993; Rye et al., 1991). Rocks altered by this process may loose half of their original mass to fluid (Gifkins et al., 2005; Hayba et al., 1985), leading to variable enrichment in immobile trace elements.

However, the uniformitarian view on the chemistry of altering fluid that caused the formation of the record-depleted $\delta^{18}O$ values in the earliest Paleoproterozoic may not fully apply because the levels of atmospheric oxygen was much lower than today (Bekker et al., 2004), and thus mechanisms of magmatic $SO_2$ oxidation and $H_2SO_4$ scrubbing by reducing groundwaters were clearly different. Furthermore, glacial or panglacial climate favors very low $CO_2$ in the air, followed by a period of hot-house conditions, in which rain is saturated with volcanically-produced carbonic and other acids (Hoffman and Schrag, 2000; Pierrehumbert, 2002). While these extreme climate conditions characterized the 2.4–2.3 Ga time interval, we were able to explain disilication trend by modern pH-neutral meteoric water at large water–rock ratios (Appendix).

### 4.5. The 2.45–2.4 Ga rift zones as a potential place for $\delta^{18}O$ depletion

Because the 2.4–2.45 Ga druzitic high-Mg gabbro-norite bodies, and their contact zones with the Chupa gneiss control the formation of high-Al low-$\delta^{18}O$ rocks in many localities, this fact alone suggests a genetic relationship in that the druzite bodies served as the heat engines that drove meteoric hydrothermal systems, capable of depleting upper portions of crust and country rocks in $\delta^{18}O$ and $\delta D$, similar to the classic system in Skaergaard (Taylor and Forester, 1979). The depths of emplacement for 2.4 Ga druzite bodies varied based on their layered equivalents in the Karelian craton, thus causing variable water–rock ratios at different depths and localities.

The intrusion of gabbro-noritic druzitic bodies of OIB and boninitic affinity at 2.4 Ga (Amelin et al., 1995; Sharkov et al., 1997) coincides in time with rifting that has been suggested for Karelia (Balagansky et al., 1986; Puchtel et al., 1997; Rybakov et al., 2000) as possibly a part of global superplume event. This rifting creates favorable hydrogeologic conditions for meteoric water circulation driven by geothermal heat and magmatic heat from shallow intrusions, as $\delta^{18}O$ depletion characterizes many other rift zones worldwide, such as Iceland and shallow Skaergaard layered intrusion. Because the strongly depleted, ≤26‰ $\delta^{18}O$ values require glacial melt-waters, an intracontinental rift zone that was never connected to the ~0‰ ocean should have been present between the studied northernmost (Peruselka) and southernmost (Kulezhma) localities (Fig. 1), 220 km apart, and possibly >400 km should 5.5‰ value at Kii Island be due to meteoric depletion. We thus envision a continent-wide glacial ice cap with subglacial rifting underneath at 2.4 Ga (Fig. 6).

### 4.6. Paleogeography and alternative reasons for low-$\delta^{18}O$ water values

It is conceivable that the presence of a low-$\delta^{18}O$, >220 km, Paleoproterozoic ice cap (Fig. 6) was due to the polar position of Karelia in which it resembled modern-day Greenland, or Iceland during Pleistocene glaciations (Fig. 8A). This interpretation warrants testing the available paleogeographic models for the possibility of a short-lived polar excursion of Fennoscandia in Paleoproterozoic times. Given ultradepleted, ≤26‰ values, a prolonged intracontinental vapor transport across a large continent or superconinent (Fig. 8B) would not suffice: waters in Lake Baikal for example are −17‰ (Wickham et al., 1996). Additionally, the interpretation shown in Fig. 8B is unlikely because 2.4–1.8 Ga is a period between supercontinents (Condie et al., 2009; Zhao et al., 2002), and the total amount of continental crust and subaerial land was likely lower in the Paleoproterozoic than today. An alpine, or intermontaine glaciation is also uncapable of

[2] The synmetamorphic fluids were initially low but temporally increased their $\delta^{18}O$ values, leading to higher $\delta^{18}O$ plagioclasites, and almost normal $\delta^{18}O$ pegmatites (Table 1). Examples of higher-$\delta^{18}O$ fluids during retrogressive stages of Svecofennian metamorphism that are seen to substitute the inferred peak metamorphic assemblage (retaining the lowest $\delta^{18}O$ values), are provided by sample B53 (Varatskoye) where −19.2‰ giant garnet is substitutes +8.6‰ amphibole; Mt. Dyadina, in sample DG121 where +10‰ magnesite substitutes +2‰ rock and has typical mantle −7‰ $\delta^{13}C$ value; sample DG16 where secondary quartz with higher $\delta^{18}O$ substitutes the original low-$\delta^{18}O$ assemblage. Finally, plagioclasite is seen as texturally developing over the high-Al rocks in Khitostrov these rocks are several to 10‰ higher; it is likely (like is the case with pegmatite X401) that the initially normal to high $\delta^{18}O$ fluids got lowered by the interaction with the ultra depleted in $\delta^{18}O$ rocks they are seen to substitute.

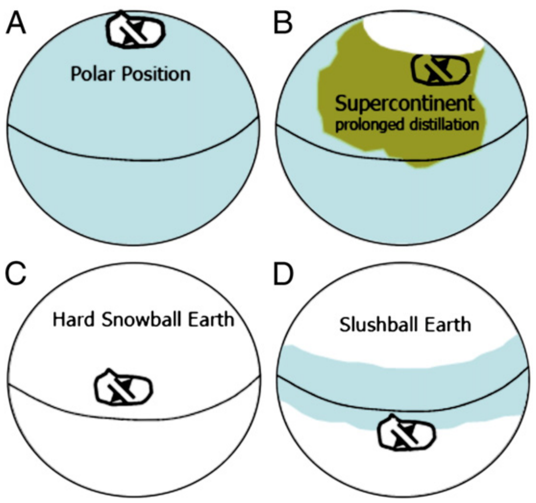


**Fig. 8.** Subglacial rifting under different paleogeogrphic and climate conditions. A) Polar position under an ice cap (Greenland-like continent). B) Position in the middle of a large supercontinent at high latitudes (e.g., Lake Baikal or NE Siberia). C) Low latitude position under "hard-Snowball" Earth climate conditions when oceans were frozen shutting down vapor–liquid isotope distillation cycle. D) Low-latitude position under "Slushball" Earth conditions in which oceans remain unfrozen to permit $\delta^{18}O$ vapor distillation onto the continent. Scenarios a and d can explain ultra-low-$\delta^{18}O$ value in Karelian rocks, but current paleomagnetic and paleogeographic reconstruction are consistent with scenario d only.

generating ≤26‰ waters, (snow in the Himalayas is −10 to −15‰ www.waterisotope.org).

Origin of $\delta^{18}O$ depletions as a result of a weathering process, and thus enrichment in Al, as is observed in bauxites, is unlikely for two reasons: (1) At low earth surface temperatures of 0º to 20 °C, isotope fractionations are large (e.g., $\Delta^{18}O$(water-kaolinite) = −26 to −29‰, Savin and Lee, 1988). The −27‰ values of rocks would correspond to ≤52‰ waters. We are unaware of any report of low-$\delta^{18}O$ bauxites worldwide. (2) Weathering occurring during ≤20 °C estimated annual climate is impossible, especially under a glacier.

Finally, if seawater was initially low in $\delta^{18}O$, (ca −10‰, as being proposed specifically for 2.0 Ga, Burdett et al., 1990), intracontinental water distillation and glaciation would still be required to explain the extreme ≤26‰ to −35‰ $\delta^{18}O$ water values. A fortuitous combination of several processes happening at once: higher elevation, mid-latitude location of Karelia, location on the polar side of a larger continent (Fig. 8b), and −10‰ initial seawater may collectively produce ≤26‰ to −35‰ $\delta^{18}O$ ice, but we consider such combination of unrelated events fortuitous, especially given large >220 km-wide isotope depletion that we discovered.

### 4.7. Evidence for a Slushball Earth?

While polar position may represent a plausible explanation of the ultra-low-$\delta^{18}O$ values, currently available paleogeographic reconstructions require a low-latitude position with more profound global implications. Combined paleomagnetic and geochronologic data suggest that Karelia was located near the equator during most of the Paleoproterozoic: at 2.22, 2.06 and 1.88 Ga, and at 2.4 Ga, in particular (Evans and Pisarevsky, 2008; Mertanen et al., 2006). As evidenced by the low-latitude, Paleoproterozoic Huronian-age (time-equivalent to the Sariolian) sequences worldwide, this time is characterized by at least three global glacial events (Bekker, in press; Bekker et al., 2004; Evans et al., 1997; Hoffman, 2009).

Bekker et al. (2004) and Hanna et al. (2004) determined that the age of the last glacial event was around 2.32 Ga, and the geological and geochemical data from this investigation suggest that the extreme $^{18}O$-depletion in and around mafic intrusions in Karelia (regionally-dated ~2.40–2.45 Ga) record an earlier Paleoproterozoic Huronian ice age. We thus envision that Karelia was in subglacial rifting conditions at low latitudes at this time (Fig. 8C and D).

Bindeman et al. (2010) suggested that the 'Slushball-Earth' model is more appropriate than the 'Hard-Snowball' model (Fig. 8C) because it allows for intracontinental vapor distillation to achieve ultra-low-$\delta^{18}O$ values in meteoric precipitation. The new findings of this work of rather extensive $\delta^{18}O$ depletion spanning >220 km, could be interpreted to represent a Karelia-wide, i.e. continental in scale, ice cap (Fig. 8). Since most $\delta^{18}O$ depletion is happening in the center, this may indirectly support the lowest $\delta^{18}O$ values resulting from vapor distillation toward the center of Karelia, like in modern Greenland.

The climate stability and the albedo effects of the hard Snowball vs. Slushball have been discussed (Bendsen, 2002; Hoffman, 2009; Lucarini et al., 2010) and questioned. Current climate models suggest that if 2/3 of the high latitude surface is frozen, the runaway effect will lead to a hard Snowball Earth outcome (www.snowballearth.org). Discussion of the climate stability models is far beyond the scope of this paper, but the data that we have presented for the Belomorian Belt, Karelia may provide support that the climate was stable in at least this part of the world during the Paleoproterozoic.

## Acknowledgements

We thank NSF grants EAR-1049351 and EAR-CAREER 0805972 for funding, Denis Korpechkov and Slava Komarov for help during fieldworks of 2008 and 2010, Jim Palandri for assistance in the lab, S.Svetov for sharing 2.4 Ga basalt sample, David Evans for on-going collaboration on Karelian paleogeography, William Peck and Andrey Bekker for very insightful and thorough reviews and for help with retrogression program, Kathryn Watts for editorial comments, to Axel Schmitt for ongoing collaboration on zircon research at UCLA National ion microprobe facility, supported by the IF-EAR NSF grant.

## Appendix A. Supplementary data

Supplementary data to this article can be found online at doi:10.1016/j.epsl.2011.03.031.

## References

Amelin, Y.V., Heaman, L.M., Semenov, V.S., 1995. U-Pb geochronology of layered mafic intrusions in the eastern Baltic Shield—implications for the timing and duration of Paleoproterozoic continental rifting. Precamb. Res. 75, 31–46.
Anderson, A.T., 1967. Dimensions of oxygen isotopic equilibrium attainment during prograde metamorphism. J. Geol. 75, 323–333.
Bekker, A., 2010. Encyclopedia of Astrobiology, Springer-Verlag, in press
Bekker, A., Holland, H.D., Wang, P.-L., Rumble 3rd., D., Stein, H.J., Hannah, J.L., Coetzee, L.L., Beukes, N.J., 2004. Dating the rise of atmospheric oxygen. Nature 427, 117–120.
Bendsen, J., 2002. Climate sensitivity to changes in solar insolation in a simple coupled climate model. Climate Dyn. 18, 595–609.
Balagansky, V.V., Bogdanova, M.N., Kozlova, N.E., 1986. Evolution of Northwest Belomorian Belt: USSR Academy of Sciences, Kola Filial, Apatity. [in Russian].
Bibikova, E.V., Bogdanova, S.V., Glebovitsky, V.A., Claesson, S., Skiold, T., 2004. Evolution of the Belomorian Belt: NORDSIM U-Pb zircon dating of the Chupa paragneisses, magmatism, and metamorphic stages. Petrology 12, 195–210.
Bibikova, E.V., Claesson, S., Glebovitsky, V.A., Sedova, I.S., Ruchev, A.M., 2001. Isotope dating of the Svecofennian metamorphism of the Belomorian belt, Baltic Shield. Geokhimia 10, 1116–1119 [in Russian].
Bibikova, E.V., Skiold, T., Bogdanova, S.V., Drugova, G.M., Lobach-Zhuchenko, S.B., 1994. Belomoride Geochronology: interpretation of multi-stage history. Geokhimia 10, 1393–1411 [in Russian].
Bindeman, I.N., 2008. Oxygen isotopes in mantle and crustal magmas as revealed by single crystal analysis. Rev. Mineral. Geochem. 69, 445–478. doi:10.2138/rmg.2008.69.12.
Bindeman, I.N., Schmitt, A.K., Evans, D.A.D., 2010. Origin of the lowest-known $\delta^{18}O$ silicate rock on Earth in Paleoproterozoic Karelian rift. Geology 38, 631–634.
Bindeman, I.N., Brooks, C.K., McBirney, A.R., Taylor, H.P., 2008. The Low-$\delta^{18}O$ late-stage ferrodiorite magmas in the Skaergaard Intrusion: result of liquid immiscibility, Thermal metamorphism, or meteoric water incorporation into magma? J. Geol. 116, 571–586.
Bindeman, I.N., Ponomareva, V.V., Bailey, J.C., Valley, J.W., 2004. Kamchatka Peninsula: a province with high-$\delta^{18}O$ magma sources and large scale $^{18}O/^{16}O$ depletion of the upper crust. Geochim. Cosmochim. Acta 68, 841–865.
Blattner, P., Grindley, G.W., Adams, C.J., 1997. Low-$^{18}O$ terrains tracking Mesozoic polar climate in the southern Pacific. Geochim. Cosmochim. Acta 61, 569–576.

Burdett, J.W., Grotzinger, J.P., Arthur, M.A., 1990. Did major changes in the stable isotope composition of Proterozoic seawater occur? Geology 18, 227–230. doi:10.1130/0091-7613(1990) 018<0227:DMCITS>2.3.CO;2.

Condie, K.C., O'Neill, C., Aster, R.C., 2009. Evidence and implications for a widespread magmatic shutdown for 250 My on Earth. Earth Planet Sci. Lett. 282, 294–298.

Criss, R.E., Taylor, H.P., 1986. Meteoric-hydrothermal systems. Rev. Mineral. 16, 373–424.

Dallai, L., Ghezzo, C., Longinelli, A., 2001. Fossil hydrothermal systems tracking Eocene climate change in Antarctica. Geology 29, 931–934.

Dansgaard, W., 1964. Stable isotopes in precipitation. Tellus 16, 436–468.

Eiler, J.M., Baumgartner, L., Valley, J.W., 1994. Intercrystalline stable isotope diffusion: a fast grain boundary model. Contrib. Mineral. Petrol. 112, 543–557.

Evans, D.A.D., Pisarevsky, S.A., 2008. Plate tectonics on the early Earth? Weighing the paleomagnetic evidence. In: Condie, K., Pease, V. (Eds.), When Did Plate Tectonics Begin? : Geological Society of America Special Paper, 440, pp. 249–263.

Evans, D.A.D., Beukes, N.J., Kirschvink, J.L., 1997. Low-latitude glaciation in the Paleoproterozoic era. Nature 386, 262–266.

Gifkins, C., Herrmann, W., Large, R., 2005. Altered Volcanic Rocks: A Guide to Description and Interpretation. University of Tasmania Publisher. 275 pp.

Giuliani, G., Fallick, A.E., Garnier, V., France-Lanord, C., Ohnenstetter, D., Schwarz, D., 2005. Oxygen isotope composition rubies and as a tracer for the origins of sapphires. Geology 33, 249–252.

Hanna, J.L., Bekker, A., Stein, H.J., Markey, R.J., Holland, H.D., 2004. Primitive Os and 2316 Ma age for marine shale: implications for Paleoproterozoic glacial events and the rise of atmospheric oxygen. Earth Planet. Sci. Lett. 225, 43–52.

Hattori, K., Muelenbachs, K., 1982. Oxygen isotopic ratios of Icelandic crust. J. Geophys. Res. 87, 6559–6565.

Hayba, D.O., Bethke, Ph.M., Heald, P., Foley, N.K., 1985. Geologic, mineralogic, and geochemical characteristics of volcanic-hosted epithermal deposits. In: Berger, B.R., Bethke, P.M. (Eds.), Geology and Geochemistry of Epithermal Systems: Rev. Econ. Geol., 2, pp. 129–168.

Hoefs, J., 2005. Stable Isotope Geochemistry, 5th edition. Springer.

Hoffman, P.F., 2009. Pan-glacial—a third state in the climate system. Geol. Today 25, 100–107. doi:10.1111/j.1365-2451.2009.00716.x.

Hoffman, P.F., Schrag, D.P., 2000. Snowball Earth. Sci. Am. 282, 68–75.

Jouzel, J., Koster, R.D., Suozzo, R.J., Russel, G.L., 1994. Stable isotope behavior during the last glacial maximum: a general circulation model analysis. J. Geophys. Res 99, 25791–25801.

Krylov, D.P., Glebovitsky, V.A., 2007. Oxygen isotopic composition and nature of fluid during formation of high-Al corundum-bearing rocks of Mt. Dyadina, Northern Karelia. Dokl. Earth Sci. 413, 210–212.

Krylov, D.P., 2008. Anomalous ratios of 18O/16O in corundum-bearing rocks from Northern Karelia. Dokl. Earth Sci. 419, 533–536.

Lobach-Zhuchenko, S.B., Bibikova, E.V., Drugova, G.M., Volodichev, O.I., Chekulaev, V.P., Krylov, I.N., Gracheva, T.B., Makarov, V., 1995. Archean magmatism of the Notozero area, NW Belomorian Belt: isotope geochronology and petrology. Petrology 3, 593–621.

Lucarini, V., Fraedrich, K., Lunkeit, F., 2010. Thermodynamic analysis of snowball Earth hysteresis experiment: efficiency, entropy production and irreversibility. Q. J. R. Meteorolog. Soc. 136, 2–11.

Masago, H., Rumble, D., Ernst, W.G., Parkinson, C.D., Maruyama, S., 2003. Low d18O eclogites from the Kokchetav massif, northern Kazakhstan. J. Metamorph. Geol. 21, 579–587. doi:10.1046/j.1525-1314.2003.00465.x.

Mertanen, S., Vuollo, J.I., Huhma, H., Arestova, N.A., Kovalenko, A., 2006. Early Paleoproterozoic-Archean dykes and gneisses in Russian Karelia of the Fennoscandian Shield—new paleomagnetic, isotope age and geochemical investigations. Precambrian Res. 144, 239–260. doi:10.1016/j.precamres.2005.11.005.

Miller, Yu.V., Milkevich, R.I., 1995. Tectonic cover-folded structure of the Belomorian Belt and its relations with the Karelian granite-greenschist region. Geotectonics 6, 80–92.

Myskova, T.A., Glebovitskii, V.A., Miller, Y.V., 2003. Supracrustal sequences of the Belomorian mobile belt: Protoliths, age, and origin. Stratigr. Geol. Correl. 11, 535–549 (in Russian).

O'Neil, J.R., 1968. Hydrogen and oxygen isotope fractionation between ice and water. J. Phys. Chem. 72, 3683–3684.

Ojakangas, R.W., Marmo, J.S., Heiskanen, K.I., 2001. Basin evolution of the Paleoproterozoic Karelian Supergroup of the Fennoscandian (Baltic) Shield. Sediment. Geol. 141–142, 255–285. doi:10.1016/S0037-0738(01)000793.

Peck, W.H., Valley, J.W., 2000. Genesis of cordierite - gedrite gneisses, Central Metasedimentary Belt boundary thrust zone, Grenville Province, Ontario, Canada. Can. Min. 38, 511–524.

Pierrehumbert, R.T., 2002. The hydrologic cycle in deep-time climate problems. Nature 419, 191–198.

Puchtel, I.S., Haase, K.M., Hofmann, A.W., Chauvel, C., Kulikov, V.S., Garbe-Schonberg, C.-D., Nemchin, A.A., 1997. Petrology and geochemistry of crustally contaminated komatiitic basalts from Vetrenny Belt, SW Baltic Shield: evidence for an early Proterozoic mantle plume beneath rifted Archean continental lithosphere. Geochim. Cosmochim. Acta 61, 1205–1222.

Reed, M.H., 1983. Calculation of multi-component chemical equilibria and reaction processes in systems involving minerals, gases and an aqueous phase. Geochim. Cosmochim. Acta 46, 512–528.

Ripley, E.M., Butler, B.K., Taib, N.I., 1992. Effects of devolatilization on the hydrogen isotopic composition of pelitic rocks in the contact aureole of the Duluth complex, NE Minnesota, USA. Chem. Geol. 102, 185–197.

Rumble, D., Yui, T.F., 1998. The Qinglongshan oxygen and hydrogen isotope anomaly near Donghai in Jiangsu Province, China. Geochim. Cosmochim. Acta 62, 3307–3321.

Rybakov, S.I., Golubev, A.I., Slusarev, V.D., Stepanov, V.S., Lavrov, M.M., Trofimov, N.N., 2000. Proterozoic rifts and their role in forming Belomorian Mobile Belt. Geology and ore Deposits in Karelia, Petrozavodsk. Issue 2, pp. 4–11 (in Russian).

Rye, R.O., 1993. The evolution of magmatic fluids in the epithermal environment: the stable isotope perspective. SEG Distinguished Lecture. Econ. Geol. 88, 733–753.

Rye, R.O., Bethke, P.M., Wasserman, M.D., 1991. The stable isotope geochemistry of acid sulfate alteration. Econ. Geol. 87, 225–262.

Salje, M.E., Vinogradov, D.P., Gavrilova, L.M., 1983. Fractionation of Oxygen Isotopes in Minerals of Polymetamorphic Complex of the Precambrian. Nauka Publisher, Leningrad Branch. 158p. [in Russian].

Savin, S.M., Lee, M., 1988. Isotopic studies of hydrous phillosilicates. In: Bailey, S.W. (Ed.), Hydrous Phillosilicates (exclusive of mica): Rev. Mineral., 19, pp. 189–233.

Serebryakov, N.S., Rusinov, V.L., 2004. High-T high-pressure Ca, Na metasomatism and formation of corundum in the pre Cambrian Belomorian mobile belt. Dokl. Earth Sci. 395, 549–533, section.

Serebryakov, N.S., 2004. Petrology of corundum-bearing rocks of the Chupa sequence of Belomorian Mobile Belt. Dissertation of the Candidate of Science, Russian State Library, 208 pp. [in Russian].

Serebryakov, N.S., Astafiev, B.Y., Voinova, O.A., Presnyakov, S.L., 2007. First single zircon dating of metasomatites from the Belomorian Belt. Dokl. Earth Sci. section 413A, 388–392.

Serebryakov, N.S., Aristov, V.V., 2004. Conditions of localization of gem-quality corundum in rocks of Chupa sequence of the Belomorian complex of Northern Karelia. Izvestiia Visshikh Uchebnikh Zavedenii. Geol. I Razvedka 4, 36–42 [in Russian].

Sharkov, E.V., Smolkin, V.F., Krassivskaya, I.S., 1997. Early Proterozoic igneous province of siliceous high-Mg boninite-like rocks in the eastern Baltic Shield. Petrology 5, 448–465.

Skublov, S.G., Balashov, Yu.A., Marin, Yu.B., Berezin, A.V., Melnik, A.E., Paderin, I.P., 2010. U-Pb age and geochemistry of zircons in Salmin eclogites (deposit Kuru-Vaara, Belomorian Belt). Doklady 432, 668–675 (in Russian).

Spicher, N.F., Reed, M.H., 1989. CHILLER: A Program for Computing Water-rock Reactions, Boiling and Mixing and other Reaction Processes in Aqueous-mineral-gas Systems, Manual. Dept. Geol. Sci, Univ. Oregon.

Stepanov, V.S., 1981. Precambrian Basic Magmatism of the Western Belomorian Belt, Leningrad. Nedra press. (monograph in Russian).

Stepanova, A.I., Larionov, A.N., Bibikova, E.V., Stepanov, V.S., Slabunov, A.I., 2003. Early Proterozoic (2.1 Ga) Fe-tholeitic magmatism of the Belomorian Province, Baltic Shield: geochemistry and geochronology. Dokl. Earth Sci. section 390, 607–610.

Sturchio, N.C., Keith, T.E.C., Muehlenbachs, K., 1990. Oxygen and carbon isotope ratios of hydrothermal minerals from Yellowstone drill cores. J. Volcanol. Geotherm. Res. 40, 23–37.

Svetov, S.A., Golubev, A.I., Svetova, A.I., 2004. Geochemistry of Sumian Basaltic Andesites of Central Karelia. Geokhimia 42, 630–640.

Taran, Yu.A., Pokrovsky, B.G., Glavatskikh, S.F., 1988. Isotope data on hydrothermal transformation of rocks in the Mutnovsky geothermal system. Kamchatka. Geochim. Int. 25, 203–221.

Taylor Jr., H.P., Sheppard, S.M.F., 1986. Igneous rocks: I. Processes of isotopic fractionation and isotopic systematics. Rev. Mineral. 16, 227–272.

Taylor, H.P., Forester, R.W., 1979. Oxygen and hydrogen isotope study of the Skaergaard intrusion and its country rocks—description of a 55-million-year old fossil hydrothermal system. J. Petrol. 20, 355–419.

Ustinov, V.I., Baksheev, I.A., Serebryakov, N.S., 2008. Oxygen isotopic composition of the mineral forming fluids of corundum-bearing metasomatic rocks at the Khitoostrov and Varaka mineral occurrences, N Karelia. Geokhimia 46, 1174–1177.

Valley, J.W., O'Neil, J., 1984. Fluid heterogeneity during granulite facies metamorphism in the Adirondacks: stable isotope evidence. Contrib. Mineral. Petrol. 85, 158–173. doi:10.1007/BF00371706.

Visotskii, S.V., Ignatiev, A.V., Yakovenko, V.V., Karabtsov, A.A., 2008. Anomalous light oxygen isotope composition in minerals of corundum-bearing rocks in northern Karelia. Dokl. Earth Sci. 423, 1216–1219. doi:10.1134/S1028334X08080072.

Wickham, S.M., Alberts, A.D., Zanvilevich, A.N., Litvinovsky, B.A., Bindeman, I.N., Schauble, E.A., 1996. A stable isotope study of anorogenic magmatism in East Central Asia. J. Petrol. 37, 1068–1095.

Zhao, G.C., Cawood, P.A., Wilde, S.A., Sun, M., 2002. Review of global 2.1–1.8 Ga orogens: implications for a pre-Rodinia supercontinent. Earth Sci. Rev. 59, 125–162. doi:10.1016/S0012-8252(02)00073-9.

Zheng, Y.-F., Wu, Y.-B., Chen, F.K., Gong, B., Li, L., Zhao, Z.-F., 2004. Zircon U-Pb and oxygen isotope evidence for a large-scale 18O depletion event in igneous rocks during the Neoproterozoic. Geochim. Cosmochim. Acta 68, 4145–4165. doi:10.1016/j.gca.2004.01.007.